Available online at www.sciencedirect.com
ScienceDirect
Desalination 219 (2008) 89–100
DESALINATION
www.elsevier.com/locate/desal

Photocatalyzed *N*-de-ethylation and degradation of Brilliant Green in TiO_2 dispersions under UV irradiation

Chiing-Chang Chen[a*], Chung-Shin Lu[a], Huan-Jung Fan[b], Wen-Hsin Chung[c], Jeng-Lyan Jan[b], Hsiu-De Lin[b], Wan-Yu Lin[c]

[a]*Department of General Education, National Taichung Nursing College, Taichung 403, Taiwan, ROC*
Tel. +886 (4) 2219-6975; Fax: +886 (4) 2219-4990; email: ccchen@ntcnc.edu.tw
[b]*Department of Environmental Engineering, Hungkuang University, Taichung 433, Taiwan, ROC*
[c]*Department of Plant Pathology, National Chung Hsing University, Taichung 402, Taiwan, ROC*

Received 6 March 2006; Accepted 17 May 2007

Abstract

The photocatalytic degradation of Brilliant Green (BG, Bis(4-diethylaminophenyl)phenylmethylium chloride), a cationic dye, was investigated in an irradiated TiO_2 aqueous dispersion. In this study, in order to obtain a better understanding on the mechanistic details of this TiO_2-assisted photodegradation of the BG dye with UV irradiation, four intermediates of the process were separated, identified, and characterized by HPLC-PDA-ESI-MS technique. The results indicated that the *N*-de-ethylation degradation of BG dye took place in a stepwise manner to yield mono-, di-, tri-, and tetra-*N*-de-ethylated BG species generated during the processes. The photodegradation of the BG dye featured competitive reactions between *N*-de-ethylation and cleavage of the BG chromophore ring structure at different pH values. However, most of all, the higher degradation rate at acid pH was observed for the cationic dyes of triphenylmethane of TiO_2-mediated experiments for the first time. These results should be useful for future applications of the treatment technology to dye pollution.

Keywords: Brilliant Green; Dye; Photocatalytic; TiO_2; *N*-de-ethylation

1. Introduction

It is reported that 10–20% of dyes are lost to wastewater as a result of inefficiency in the dyeing process [1]. Dyestuffs from the textile and photographic industries are becoming a major source of environmental pollution. The large amount of dyestuffs used in the dyeing stage of textile manufacturing processes represents an increasing environmental danger due to their refractory carcinogenic nature [2]. To de-pollute the dyeing wastewater, a number of methods have been investigated including chemical oxidation

*Corresponding author.

0011-9164/08/$– See front matter
doi:10.1016/j.desal.2007.05.009

and reduction, chemical precipitation and flocculation, photolysis, adsorption, ion pair extraction, electrochemical treatment, and advanced oxidation [3].

The advanced oxidation process (AOP) is one of the most promising technologies for the removal of dye-contaminated wastewaters due to its high efficiency. This technology is mainly based on the oxidative reactivity of HO• radicals generated by various methods like O_3/UV, H_2O_2/UV, H_2O_2/Vis, O_3/H_2O_2/UV photolysis, photo-assisted Fe^{3+}/H_2O_2, and TiO_2-mediated photocatalysis processes.

The TiO_2-mediated photocatalysis process has been successfully used to degrade pollutants during the past few years [4–11]. TiO_2 is broadly used as a photocatalyst because of its nontoxicity, photochemical stability and low cost [12]. The initial step in the TiO_2-mediated photocatalysis degradation is proposed to involve the generation of a (e^-/h) pair leading to the formation of hydroxyl radicals (•OH), superoxide radical anions (O_2^-) and hydroperoxyl radicals (•OOH), and these radicals are the oxidizing species in the photocatalytic oxidation processes. The efficiency of the dye degradation depends on the concentration of the oxygen molecules, which either scavenge the conduction band electrons (e^-_{cb}) or prevent the recombination of (e^-/h^+). The electron in the conduction band can be picked up by the adsorbed dye molecules, leading to the formation of dye radical anions and the degradation of the dye [13].

Triphenylmethane dyes are used extensively in the textile industry for dyeing nylon, wool, cotton, and silk, as well as for coloring of oil, fats, waxes, varnish, and plastics. The paper, leather, cosmetic, and food industries consume a high quantity of triphenylmethane dyes of various kinds [1]. Additionally, the triphenylmethane dyes are applied as staining agents in bacteriological and histopathological applications. The photocytotoxicity of triphenylmethane dyes, based on the production of the reactive oxygen species, is tested intensively with regard to their photodynamic treatment [14,15]. However, there is a great concern about the thyroid peroxidase-catalyzed oxidation of the triphenylmethane class of dyes because the reactions might form various *N*-de-alkylated primary and secondary aromatic amines, which have structures similar to aromatic amine carcinogens [16].

In earlier reports [17–19], the photodegradation of the triphenylmethane dyes were investigated. The *N*-de-alkylation process was predicated on the basis of the wavelength shift of maximal absorption of the dyes. However, only a portion of the *N*-de-alkylation intermediates of these dyes has been isolated and identified under UV irradiation.

Therefore, this research focused on the identification of the *N*-de-ethylation intermediates of BG to investigate the mechanistic details of the *N*-de-ethylation of BG dye in the TiO_2/UV light process.

2. Experimental

2.1. Materials

Titanium dioxide was Degussa P-25, and it was in the anatase form (ca. 80% anatase, 20% rutile). It had a BET surface area of 50±15 m^2/g and an average particle diameter of 21 nm, containing 99.5% TiO_2. BG dye was obtained from Tokyo Kasei Kogyo and used without any further purification. The chemical structure of the BG dye is shown in Fig. 1. Stock solutions containing 1 g/L of BG dye in water were prepared, protected from light, and stored at 4°C. HPLC analysis was employed to confirm the presence of the BG dye as a pure organic compound.

Reagent-grade ammonium acetate, sodium hydroxide, nitric acid, and HPLC-grade methanol were purchased from Merck. De-ionized water was used throughout this study. The water was then purified with a Milli-Q water ion-exchange system (Millipore Co.) to give a resistivity of 1.8×10^7 Ω-cm.

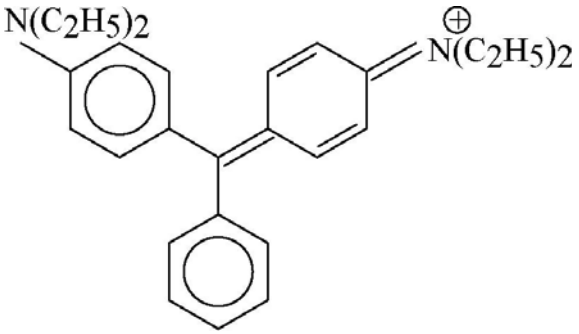

Fig. 1. Chemical structure of Brilliant Green.

2.2. Instruments

A Waters ZQ LC/MS system—equipped with a binary pump, photodiode array detector, autosampler, and micromass detector—was used for separation and identification. The C-75 Chromato-Vue cabinet of UVP provides a wide area of illumination from the 15-Watt UV-365 nm tubes positioned on two sides of the cabinet interior.

2.3. Procedures and analysis

An aqueous TiO_2 dispersion was prepared by adding 50 mg of TiO_2 powder to a 100 mL solution containing the BG dye at appropriate concentrations. For reactions in different pH media, the initial pH of the suspensions was adjusted by addition of either NaOH or HNO_3 solutions. Prior to irradiation, the dispersions were magnetically stirred in the dark for ca. 30 min to ensure the establishment of the adsorption/desorption equilibrium. Irradiations were carried out using two UV-365 nm lamps (15 Watt). At any given irradiation time interval, the dispersion was sampled (5 mL), centrifuged, and subsequently filtered through a Millipore filter (pore size, 0.22 μm) to separate the TiO_2 particles.

After each irradiation cycle, the amount of the residual dye was thus determined by HPLC. The analysis of organic intermediates was accomplished by HPLC-ESI-MS after the readjustment of the chromatographic conditions in order to make the mobile phase compatible with the working conditions of the mass spectrometer. Two different kinds of solvents were prepared in this study. Solvent A was 25 mM aqueous ammonium acetate buffer (pH 6.9) while solvent B was methanol instead of ammonium acetate. LC was carried out on an Atlantis™ dC18 column (250 mm×4.6 mm i.d., dp = 5 μm). The flow rate of the mobile phase was set at 1.0 mL/min. A linear gradient was set as follows: t = 0, A = 95, B = 5; t = 20, A = 50, B = 50; t = 55, A = 10, B = 90; t = 60, A = 95, B = 5. The column effluent was introduced into the ESI source of the mass spectrometer. Equipped with an ESI interface, the quadruple mass spectrometer with heated nebulizer probe at 350 °C was used with an ion source temperature of 80 °C. ESI was carried out with the vaporizer at 350 °C and nitrogen as sheath (551 kPa) and auxiliary (138 kPa) gas to assist with the preliminary nebulization and to initiate the ionization process. A discharge current of 5 μA was applied. Tube lens and capillary voltages were optimized for the maximum response during perfusion of the BG standard.

Performed in flask without addition of TiO_2, the blank experiments show no appreciable decolorization of the irradiated solution, thus confirming the expected stability of this BG dye under UV light irradiation. Also, with addition of 0.5 g/L TiO_2 to solution, which contains 50 mg/L of the BG dye, the stability of the dye was not altered in the dark either.

3. Results and discussion

3.1. pH effect

The point of zero charge (pzc) of the TiO_2 is at pH 6.8 [20]. The TiO_2 surface is predominantly negatively charged when the pH is higher than the TiO_2 isoelectric point. As the pH decreases, the functional groups are protonated, and the proportion of the positively charged surface

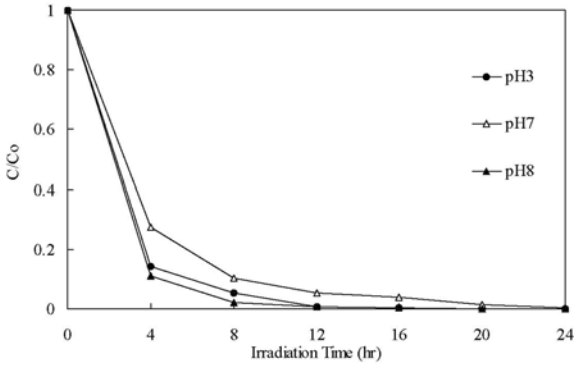

Fig. 2. pH effect on the BG photodegradation rate with concentrations of TiO_2 to be 0.5 g/L and BG to be 0.05 g/L.

increases. Thus, the electrical property of the TiO_2 surface varies with the pH of the dispersion. The surface of TiO_2 would be negatively charged in the alkaline media (pH>6.8) and adsorb cationic species easily while under acidic conditions (pH<6.8) it would adsorb anionic ones. However, pH changes can thus influence the adsorption of dye molecules onto the TiO_2 surfaces, an important step for photocatalytic oxidation to take place.

The photodegradation rate of the BG dye as a function of reaction pH is shown in Fig. 2. The photodegradation rate of the BG dye was found to decrease then increase with the increase in the value of pH. Under acidic conditions, if we compare spectrum 1 with spectrum 2 in Fig. 3a, it was found that the cationic BG dye was difficult to adsorb onto the TiO_2 surface. Active $^{\bullet}OH$ radicals formed at low concentrations and hence the photodegradation process of BG remained slow. However, an observation of the pH 3 curve of Fig. 2 and of spectrum 2 in Fig. 3a shows that the photodegradation rate of BG was actually fast. The results of photodegradation rate is different from that was found with the cationic dyes of the triphenylmethane/TiO_2 system [18, 21–23]. Moreover, a higher degradation rate at acid pH is seen also for the degradation of azo

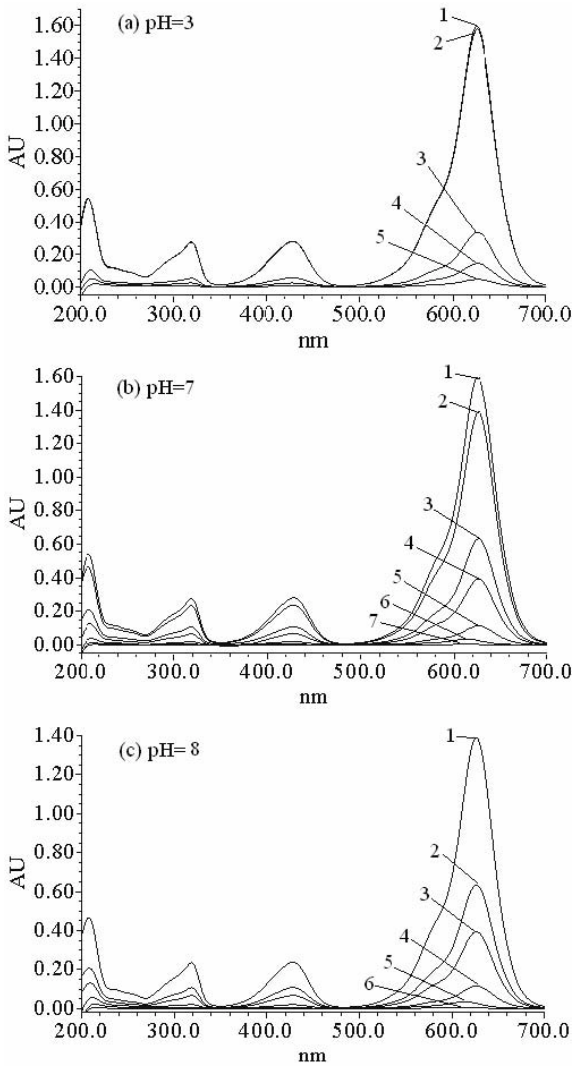

Fig. 3. UV-visible spectra changes of the BG dye in aqueous TiO_2 dispersions (BG 0.05 g/L, TiO_2 0.5g/L) as a function of the irradiation time. (a) Spectra 2–5 denote the irradiation times of 0, 4, 8, and 12 h, respectively. (b) Spectra 2–7 denote the irradiation times of 0, 4, 8, 12, 16, and 20 h, respectively. (c) Spectra 2–6 denote the irradiation times of 0, 4, 8, 12, and 16 h, respectively. Spectrum 1 is the UV-visible spectrum of BG before addition of particulates to the solution.

dyes in TiO_2-mediated experiments due to the efficient electron-transfer process that occurs with surface complex bond formation [24,25].

Hydroxyl radicals can be formed by the reaction between hydroxide ions and positive holes. The positive holes are considered major oxidation species at low pH while hydroxyl radicals are the predominant species at neutral or high pH levels [26]. An additional explanation for the pH effects is related to changes in the specification of the dye. That is, protonation or deprotonation of the dye can change its adsorption characteristics and redox activity [27]. In the presence of TiO_2 particles, the absorbance decreases very little (Fig. 3a, spectrum 2), reflecting the extent of the adsorption of BG on the TiO_2 surface in the dark. However, the data of Fig. 3a indicate only a decrease in absorbance with irradiation time and no peak wavelength shifts. We deduce that no *N*-de-ethylation of BG takes place under these conditions and that only degradation of the aromatic chromophore takes place relatively rapidly, in less than 12 h. Thus, when TiO_2 is added to the solutions, reactions analogous to the efficient electron-transfer process can take place by strong surface complex bond formation and produce $^{\bullet}OH$ radicals by the reaction between hydroxide ions and positive holes. Such reactions also attack BG, but principally at the aromatic chromophore, leading to degradation of the BG structure rather than to *N*-de-ethylation.

Under neutral pH values, when comparing spectrum 1 with spectrum 2 in Fig. 3b, one can observe that the cationic BG dye was much easier to adsorb onto the TiO_2 surface. However, this surface is not easily charged, and the photodegradation of BG became therefore slower.

With higher pH values, the formation of active $^{\bullet}OH$ species is favored, due not only to improved transfer of holes to the adsorbed hydroxyls, but also to electrostatic abstractive effects between the negatively charged TiO_2 particles and the operating cationic dyes (Fig. 3c). Hence, the photodegradation of BG was the fastest (Fig. 2, pH 8 curve). Our results indicate that the TiO_2 surface is negatively charged, and the BG adsorbs onto the TiO_2 surface through the positive ammonium groups. The proposed adsorption mechanisms are in good agreement with earlier reports [28]. In the presence of TiO_2 particles, the absorbance decreases a lot (Fig. 3c, spectrum 2), reflecting the extent of the adsorption of BG on the TiO_2 surface in the dark. However, the data of Fig. 3c indicate a decrease in absorbance with irradiation time and peak wavelength shifts at 12 h. Examination of the spectral variation of Fig. 3c suggests that the *N*-de-ethylation of BG seems to predominate and the cleavage of the BG chromophore structure occurs only to a slight extent, as confirmed by decreases in the gradual peak intensities following the wavelength shift. The proposed mechanisms and wavelength shift are in good agreement with earlier reports [21, 29–30]. Although the BG dye can adsorb onto the TiO_2 surface to some extent in alkaline media, when the pH value is too high (pH = 9), the BG dye molecules will change into a leuco-compound.

3.2. UV-visible spectra

The aqueous solution of the BG dye was a little unstable under UV radiation in absence of TiO_2. However, the BG dye can be degraded efficiently in aqueous BG/TiO_2 dispersions by UV irradiation at wavelength 365 nm. At different pH values, the changes in the UV-visible spectra during the BG dye photodegradation process in the aqueous TiO_2 dispersions under UV irradiation are illustrated in Fig. 3. The BG dye shows a major absorption band at 626.3 nm (spectrum 1). UV-light irradiation of the aqueous BG/TiO_2 dispersion leads to a decrease in absorption with a concomitant wavelength shift of the band to shorter wavelengths, reminiscent of similar hypsochromic shifts seen by Wu et al. [31] in the RhB/CdS system illuminated at $\lambda >$ 540 nm. During the BG dye photodegradation period, competitive reactions between *N*-de-ethylation and cleavage of the BG chromophore ring structure occurred. Longer irradiation by UV

light leads to further formation of the *N*-de-ethylated BG intermediates as indicated by changes in the wavelength (Fig. 3b and 3c).

During UV irradiation, the characteristic absorption band of the dye around 626.3 nm decreased rapidly with slight hypsochromic shifts (615.2 nm), but no new absorption bands appeared even in the ultraviolet range (λ> 200 nm), indicating that a series of *N*-de-ethylated intermediates may have formed along with possible cleavage of the whole conjugated chromophore structure of the BG dye. Moreover, with the irradiation of UV-light for 20 h, not only did the characteristic absorption band of the dye around 615.2 nm disappear (Fig. 3b), but also no new absorption bands appeared even in the ultraviolet range (200 nm <λ<400 nm), indicating possible cleavage of the whole conjugated chromophore structure of the BG dye and the degradation of the phenylic skeleton. In Fig. 3c, the results were also the same with 16 h of UV-light irradiation.

3.3. Effect of photocatalyst concentration

From both a mechanistic and application point of view, studying the dependence of the photocatalytic reaction rate on the concentration of TiO_2 in the BG dye is important. Hence, the effect of photocatalyst concentration on the photodegradation rate of the BG dye was investigated by employing different concentrations of TiO_2 varying from 0.1 to 0.5 g/L. As expected, the photodegradation rate of the BG was found to increase then decrease with the increase in the catalyst concentration (Fig. 4), a general characteristic of heterogeneous photocatalyst, and our results are in agreement with the earlier reports [21,30]. However, the scattering light is known to have a practical limit, above which the degradation rate will decrease due to the reduction of the photonic flux within the irradiated solution.

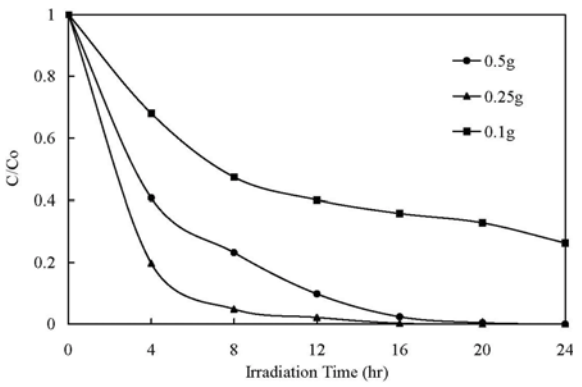

Fig. 4. Influence of the catalyst concentration on the photodegradation rate for the decomposition of BG. Experimental conditions: dye concentration (0.05 g/L), *V*=100 mL, pH 7, absorbance was recorded at 625 nm, continuous stirring, irradiation time 24 h.

3.4 Separation and identification of the intermediates

Temporal variations occurring in the solution of the BG dye during the photodegradation process with UV irradiation were examined with HPLC, coupled with a photodiode array detector and ESI mass spectrometry. The chromatogram, recorded at 600 nm, is illustrated in Fig. 5. With irradiation up to 12 h, five components were identified, all with the retention times under 55 min. We denoted the BG dye and its related intermediates as species A–E. The absorption

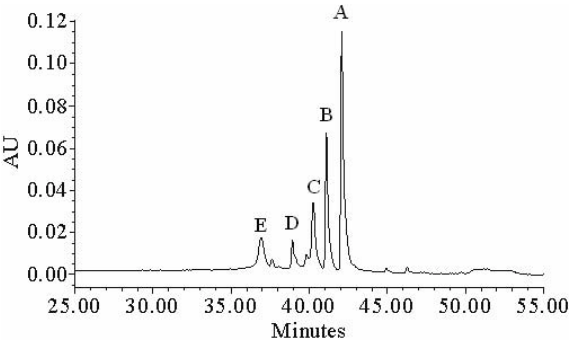

Fig. 5. HPLC chromatogram of the *N*-de-ethylated intermediates with 12 h of irradiation at pH 7, recorded at 600 nm.

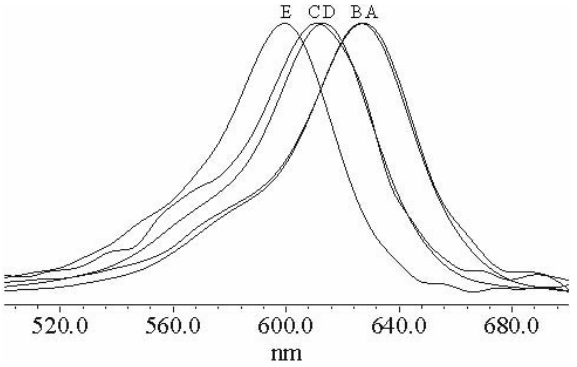

Fig. 6. Absorption spectra of the *N*-de-ethylated intermediates formed during the photodegradation process of the BG dye corresponding to the peaks in the HPLC chromatograph of Fig. 5. Spectra were recorded using the photodiode array detector. Spectra A–E correspond to the peaks A–E in Fig. 5, respectively.

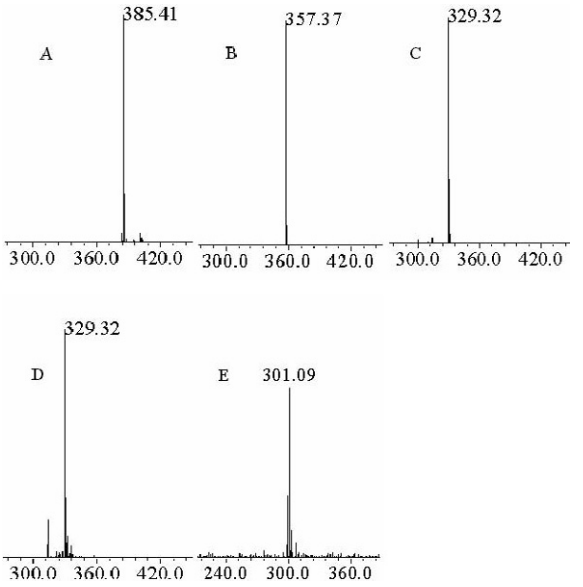

Fig. 7. ESI mass spectra of *N*-de-ethylated intermediates formed during the photodegradation of the BG dye after they were separated by HPLC method: mass spectra denoted A–E correspond to the A–E species in Fig. 5, respectively.

spectra of all intermediates in the visible spectral region are depicted in Fig. 6; they are identified as A–E (Fig. 6) and correspond to peaks A–E in Fig. 5, respectively. The absorption maximum of the spectral bands shifts hypsochromically from 628.7 nm (Fig. 6, spectrum A) to 596.3 nm (Fig. 6, Spectrum E). For example, λ_{max} of A (BG), B, C, D, and E are 628.7, 626.6, 612.2, 617.8 and 596.3 nm, respectively. This hypsochromic shift of the absorption band results presumably from the formation of a series of *N*-de-ethylated intermediates in a stepwise manner (i.e., ethyl groups are removed one by one as confirmed by the gradual peak wavelength shifts toward the blue region). Further irradiation caused the decrease of the absorption band at 596.3 nm, but no further wavelength shift was observed, implying that the band at 596.3 nm was that of the *N*-tri-de-ethylated product of BG dye. Similar phenomena were also observed during the photodegradation of rhodamine-B [19] and sulforhodamine-B [17] under visible irradiation.

The wavelength shifts depicted in Fig. 6 are due to the *N*-de-ethylation of the BG dye caused by the attacks of some active oxygen species on the *N*,*N*-diethyl and *N*-ethyl groups. This argument will be supported by the following results, and a mechanism is proposed accordingly.

The *N*-de-ethylated intermediates were further identified using the HPLC-ESI mass spectrometric method, and the relevant mass spectra are illustrated in Fig. 7. The molecular ion peaks appeared to be in the acid forms of the intermediates. Using mass spectral analysis, we confirmed that component A, m/z = 385.41, in the liquid chromatogram was BG (Fig. 7, mass spectra A); the other components were B, m/z = 357.37, (4-diethylaminophenyl)(4-ethylaminophenyl)phenylmethylium (Fig. 7, mass spectra B); C, m/z = 329.32, (4-ethylamino-phenyl)(4-ethylaminophenyl) phenylmethylium (Fig. 7, mass spectra C); D, m/z = 329.32, (4-diethylaminophenyl)(4-aminophenyl)phenylmethylium (Fig. 7, mass spectra D); and E, m/z = 301.09, (4-ethylaminophenyl)(4-amino-phenyl)phenylmethylium (Fig. 7, mass spectra E). Results of

Table 1
Identification of the *N*-de-ethylation intermediates of the BG dye by HPLC-ESI-MS

HPLC peaks	*N*-de-ethylation intermediates	Abbreviation	ESI-MS peaks (m/z)	Absorption maximum (nm)
A	Bis(4-diethylaminophenyl)phenylmethylium	DD-PM; MG	385.41	628.7
B	(4-diethylaminophenyl) (4-ethylaminophenyl)phenylmethylium	DE-PM	357.37	626.6
C	(4-ethylaminophenyl) (4-ethylaminophenyl)phenylmethylium	EE-PM	329.32	612.2
D	(4-diethylaminophenyl) (4-aminophenyl)phenylmethylium	D-PM	329.32	617.8
E	(4-ethylaminophenyl) (4-aminophenyl)phenylmethylium	E-PM	301.09	596.3
F	Bis(p-aminophenyl)phenylmethylium	PM	N/A	N/A

HPLC chromatograms, UV-visible spectra, and HPLC-ESI mass spectra are summarized in Table 1.

The relative distribution of the *N*-de-ethylated intermediates obtained is illustrated in Fig. 8. To minimize errors, the relative intensities were recorded at the maximum absorption wavelength for each intermediate, although a quantitative determination of all of the photogenerated intermediates was not achieved, owing to the lack of the appropriate molar extinction coefficients of these intermediates and the related reference standards. The distributions of all the N-de-methylated intermediates are expressed as absorbance relative to the initial concentration of BG. Nonetheless, we clearly observed the changes in the distribution of each intermediate during the photodegradation process of the BG dye. In the data of Fig. 8, the successive appearance of the maximal distribution of each intermediate indicates that the *N*-de-ethylation of BG is a stepwise photochemical process.

However, the emerging intermediates, the absorption-maximum peaks of which can be easily observed in Fig. 8, correspond to those species with several ethyl groups detached from the BG dye. Except for the initial BG dye (peak A), the intensities of the other peaks

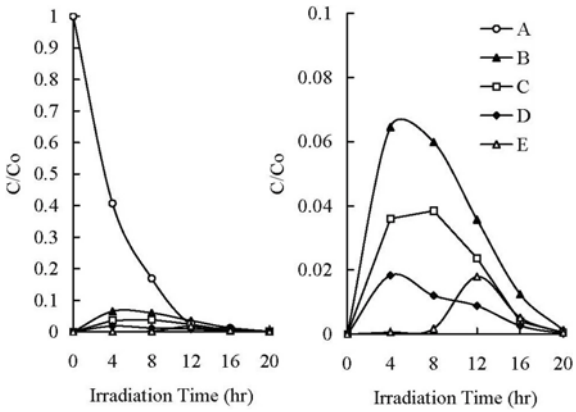

Fig. 8. Variation in the relative distribution of the *N*-de-ethylated products obtained from the photodegradation of the BG dye as a function of the irradiation time under pH 8. Curves A–E correspond to the peaks A–E in Fig. 5, respectively.

increased at first and subsequently decreased, indicating the formation and transformation of the intermediates. According to the number of the ethyl groups detached, we can characterize these intermediates. We have found a pair of isomeric molecules, i.e., di-*N*-de-ethylated BG species, different only in the way they loosen the ethyl groups from the benzyl groups. One of the di-*N*-de-ethylated BG isomers, MM-PM, is formed by the removal of the ethyl group from two different

benzyl groups of the BG molecule while the other isomer, D-PM, is produced by loosening two ethyl groups from the same benzyl group of the BG dye. Therefore, considering the polarity of the D-PM species exceeds that of the MM-PM intermediates, we expected the latter to be eluted after the D-PM species. As well, to the extent that two *N*-ethyl groups are stronger auxochromic moieties than the *N*, *N*-diethyl groups or amino group are, the maximal absorption of the D-PM intermediates could be anticipated to occur at wavelengths shorter than the band position of the MM-PM species.

Under UV irradiation, most of the $^{\bullet}OH$ radicals are generated directly from the reaction between the holes and surface-adsorbed H_2O or OH^-. The probability for the formation of $O_2^{-\bullet}$ should be much less than that of $^{\bullet}OH$ [19]. The *N*-de-ethylation of the BG dye occurs mostly by the attack of the $^{\bullet}OH$ species on the *N*,*N*-diethyl groups of the BG dye. Considering that the *N*,*N*-diethyl group in D-PM is bulkier than the *N*-ethyl group in MM-PM, molecules, the attack of $^{\bullet}OH$ radicals on the *N*-ethyl groups should be favored at the expense of the *N*,*N*-diethyl groups. In accord with this notion, the HPLC results showed that the D-PM intermediates reached maximum concentration before the MM-PM intermediates did. The *N*-di-de-ethylated intermediates (MM-PM and D-PM) were clearly observed (Fig. 8, curve C–D) to reach their maximum concentrations after 8- and 4-h irradiation periods due to the factors as mentioned above. The *N*-tri-de-ethylated intermediate (M-PM) was clearly observed (Fig. 8, curve E) to reach its maximum concentration after a 12-h irradiation period. The successive appearance of the maximal quantity of each intermediate indicates that the *N*-de-ethylation of BG is a stepwise photochemical process by de-ethylation intermediates. The results we discussed above can be seen more clearly from Fig. 9.

The *N*-mono-de-ethylated intermediates (DM-PM) and *N*-di-de-ethylated intermediates (D-PM and MM-PM) were clearly observed (Fig. 8, curve B–D), following which DM-PM degraded rapidly. A small amount of the third *N*-de-ethylated intermediate (M-PM) was also detected (Fig. 8, curve E), but the fourth *N*-de-ethylated intermediate (PM) was not detected. The first product (DM-PM) of *N*-de-ethylation reached its maximum concentration after a 4-h irradiation period (Fig. 8, curve B) while the maximum of the third *N*-de-ethylated product (M-PM) appeared after 12-h irradiation (Fig. 8, curve E). The chromophoric species (BG) was still observed even after irradiation for 20 h. During the period of the photodegradation of the BG dye, competitive reactions between *N*-de-ethylation and cleavage of the BG chromophore ring structure occurred. This indicates that the *N*-de-ethylation process predominates, and the cleavage of the conjugated structure occurs at a somewhat slower rate until four ethyl groups are removed.

When the BG dye molecules are near the TiO_2 surface due to the diethylamine group, which somewhat neutralizes the surface, the *N*-de-ethylation process predominates during the initial stages. Destruction of the chromophore ring structure occurs mostly only after full de-ethylation of the dye appears.

According to earlier reports [19,32], most oxidative *N*-de-alkylation processes are preceded by the formation of a nitrogen-centered radical while the destruction of the dye chromophore structures is preceded by generation of the carbon-centered radical [18,33–35]. To be consistent with this, the degradation of BG would have to occur via two different photooxidation pathways (destruction of the chromophore structure and *N*-de-ethylation) due to the formation of the different radicals (either carbon-centered radical or nitrogen-centered radical). There is no doubt that electron injection from the dye to the positive holes of TiO_2 yields the dye cationic radical. After this stage, the cationic radical, $dye^{\bullet+}$, can undergo the hydrolysis and/or deprotonation pathways of the dye cationic radicals,

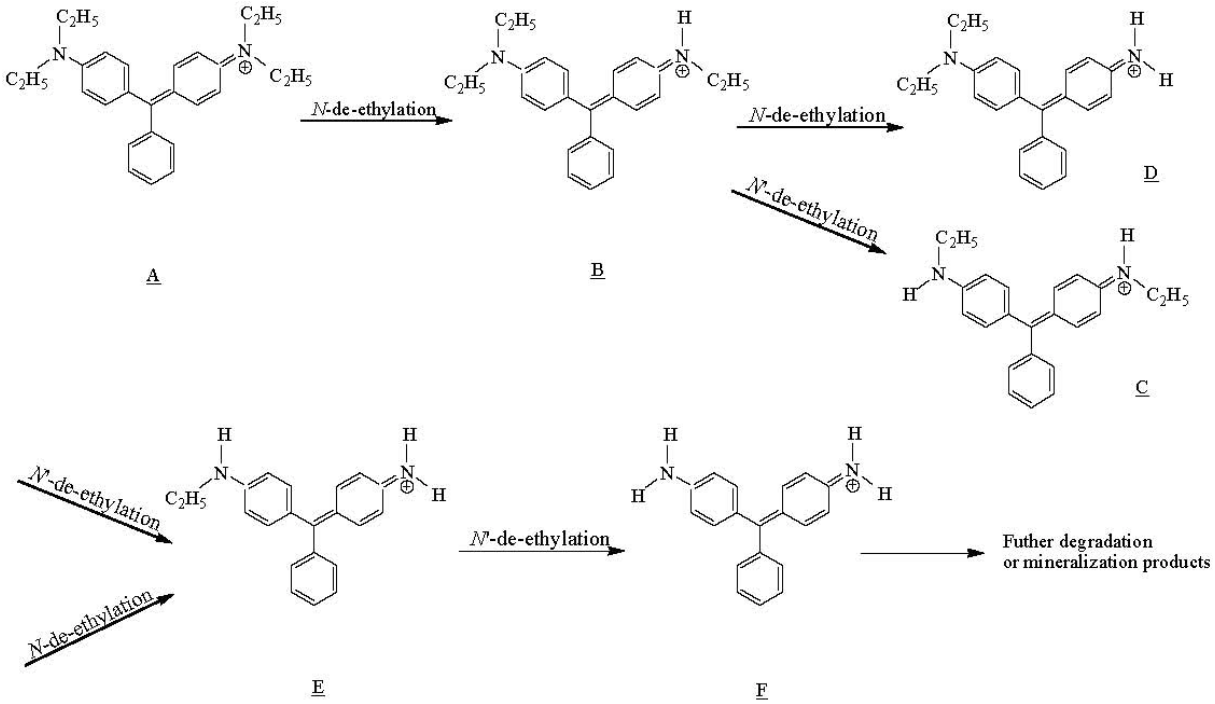

Fig. 9. Proposed *N*-de-ethylation mechanism of the BG dye under UV irradiation in aqueous TiO_2 dispersions followed by the identification of several intermediates by HPLC-ESI mass spectral techniques under pH 8.

which in turn are determined by the different adsorption modes of BG on the TiO_2 particle surface [34].

On the basis of all the above experimental results, we tentatively propose the pathway of *N*-de-ethylation as depicted in Fig. 9. The dye molecule in the BG/TiO_2 system is adsorbed through the positively charged dimethylamine groups at neutral or high pH levels. Then the $^{\bullet}OH$ radicals are attacked from the TiO_2 particle surface to the adsorbed dye through the positively charged diethylamine groups and the subsequent hydrolysis (or deprotonation) yields a nitrogen-centered radical, which is then attacked by molecular oxygen to lead ultimately to de-ethylation. The mono-*N*-de-ethylated dye, DM-PM, can also be adsorbed on the TiO_2 particle surface and be involved in the other similar events (such as $^{\bullet}OH$ radical attack, oxygen attack and hydrolysis or deprotonation) to yield a bi-*N*-de-ethylated dye derivative, D-PM and MM-PM. The *N*-de-ethylation process as described above continues until formation of the completely *N*-de-ethylated dye, PM. Moreover, the higher degradation rate at acid pH is seen also for the degradation of azo dyes of TiO_2-mediated experiments due to the efficient electron-transfer process that accompanies strong surface complex bond formation. Hydroxyl radicals can be formed by the reaction between hydroxide ions and positive holes. The positive holes are considered the major oxidation species at low pH levels while hydroxyl radicals predominate at neutral or high pH.

4. Conclusions

The BG dye could be successfully decolorized and degraded by TiO_2 under UV irradiation. Both *N*-de-ethylation and degradation of the BG dye take place in presence of TiO_2 particles. The

photodegradation rate of the BG dye was found to decrease then increase along with the increase in the value of pH. The photodegradation rate of the BG dye was found to increase then decrease along with the increase in the catalyst concentration. After 15 Watt UV-365 nm irradiation for 8 h, ca. 95.5% of BG was degraded.

The positive holes are considered the major oxidation species at low pH levels while hydroxyl radicals predominate at neutral or high pH. Under acidic conditions, we deduce that no *N*-de-ethylation of BG takes place, only degradation of the aromatic chromophore. With higher pH values, we suggest that the *N*-de-ethylation of BG seems to predominate and cleavage of the BG chromophore structure occurs only to a slight extent as confirmed by the gradual decrease in peak intensities after wavelength shift. The *N*-de-ethylation process continues until formation of the completely *N*-de-ethylated dye.

Acknowledgements

This research was supported by the National Science Council of the Republic of China (NSC 95-2113-M-438-001).

References

[1] Ullmann's Encyclopedia of Industrial Chemistry, Part A27, Triarylmethane and Diarylmethane Dyes, 6th ed., Wiley–VCH, New York, 2001.
[2] A. Reife, Dyes environmental chemistry. In: Kirk, ed., Othmer Encyclopedia of Chemical Technology, Vol. 8, 4th ed., Wiley, New York, 1993, pp. 753–784.
[3] P. Coopper, Asian Text. J., 4 (1995) 52–59.
[4] C.C. Chen, X. Li, J. Zhau, H. Hidaka and N. Serpone, J. Phys. Chem. B, 106 (2002) 318–326.
[5] N. Watanabe, S. Horikoshi, A. Kawasaki, H. Hidaka and N. Serpone, Environ. Sci. Technol., 39 (2005) 2320–2326.
[6] S.Parra, S.E. Stanca, I. Guasaquillo and K.R. Thampi, Appl. Catal. B: Environ., 51 (2004) 107–116.
[7] C.C. Chen, C.S. Lu and Y.C. Chung, J. Photochem. Photobiol. A: Chem., 181 (2006) 120–125.
[8] H. Kyung, J. Lee and W. Choi, Environ. Sci. Technol., 39 (2005) 2376–2382.
[9] H. Hidaka, H. Honjo, S. Horikoshi and N. Serpone, New J. Chem., 27 (2003) 1371–1376.
[10] C. Nasr, K. Vinodgopal, L. Fisher, S. Hotchandani, A.K. Chattopadhyap and P.V. Kamat, J. Phys. Chem. B, 100 (1996) 8436–8442.
[11] J. Lee, W. Choi and J. Yoon, Environ. Sci. Technol., 39 (2005) 6800–6807.
[12] A.L. Linsebigler, G.Q. Lu and J.T.Y. Jr, Chem. Rev., 95 (1995) 735–758.
[13] M.R. Hoffman, S.T. Martin, W. Choi and W. Bahnemann, Chem. Rev., 95 (1995) 69–96.
[14] M.S. Baptista and G.L. Indig, J. Phys. Chem. B, 102 (1998) 4678–4688.
[15] R. Bonnett and G. Martinez, Tetrahedron, 57 (2001) 9513–9547.
[16] B.P. Cho, T. Yang, L.R. Blankenship, J.D. Moody, M. Churchwell, F.A. Bebland and S. Culp, J. Chem. Res. Toxicol., 16 (2003) 285–294.
[17] C.C. Chen, W. Zhao, J.G. Li, J.C. Zhao, H. Hidaka and N. Serpone, Environ. Sci. Technol., 36 (2002) 3604–3611.
[18] I.K. Konstantinou and T.A. Albanis, Appl. Catal. B: Environ., 49 (2004) 1–14.
[19] T. Wu, G. Liu, J. Zhao, H. Hidaka and N. Serpone, J. Phys. Chem. B, 102 (1998) 5845–5851.
[20] I. Poulios, I. Tsachpinis and J. Chem. Technol. Biotechnol., 74 (1999) 349–357.
[21] C.C. Chen, F.D. Mai, K.T. Chen, C.W. Wu and C.–S. Lu, Dyes Pigments, 75 (2007) 434–442.
[22] H. Kominami, H. Kumamoto, Y. Kera and B. Ohtani, J. Photochem. Photobiol. A: Chem., 160 (2003) 99–104.
[23] Y. Bessekhouad, D. Robert and J.V. Weber, J. Photochem. Photobiol. A: Chem., 157 (2003) 47–53.
[24] J. Bandara, J.A. Mielczarski and J. Kiwi, Langmuir, 15 (1999) 7680–7687.
[25] S. Naskar, S. Arumugam and M. Chanda, J. Photochem. Photobiol. A: Chem., 113 (1998) 257–264.
[26] L. Lucarelli, V. Nadtochenko and J. Kiwi, Langmuir, 16 (2000) 1102–1108.
[27] B. Neppolian, H.C. Choi, S. Sakthivel, B. Arabin-

doo and V. Murugesan, Chemosphere, 46 (2002) 1173–1181.
[28] X. Li, G. Liu and J. Zhao, New J. Chem., 23 (1999) 1193–1196.
[29] G. Liu, X. Li and J. Zhao, Environ. Sci. Technol., 34 (2000) 3982–3990.
[30] C.C. Chen, C.S. Lu, Y.C. Chung and J.L. Jan, J. Haz. Mater., 141 (2006) 520–528.
[31] T. Watanabe, T. Takizawa and K. Honda, J. Phys. Chem., 81 (1977) 1845–1851.
[32] G. Galliani, B. Rindone and C. Scolastico, Tetrahedron Lett.,16 (1975) 1285–1288.
[33] F. C. Shaefer and W.D. Zimmermann, J. Org. Chem., 35 (1970) 2165–2174.
[34] B.L. Laube, M.R. Asirvatham and C.K. Mann, J. Org. Chem., 42 (1977) 670–674.
[35] T. Wu, J. Lin, J. Zhao, H. Hidaka and N. Serpone, Environ. Sci. Technol., 33 (1999) 1379–1387.
[36] G. Liu, T. Wu, J. Zhao, K. Wu, K. Oikawa, H. Hidaka and N. Serpone, New J. Chem., 24 (2000) 411–417.